Progress In Electromagnetics Research, Vol. 148, 159–170, 2014

Mixed Finite Element Method for 2D Vector Maxwell's Eigenvalue Problem in Anisotropic Media

Wei Jiang[1], Na Liu[1], Yifa Tang[2], and Qing Huo Liu[3, *]

Abstract—It is well known that the conventional edge element method in solving vector Maxwell's eigenvalue problem will lead to the presence of nonphysical zero eigenvalues. This paper uses the mixed finite element method to suppress the presence of these nonphysical zero eigenvalues for 2D vector Maxwell's eigenvalue problem in anisotropic media. We introduce a Lagrangian multiplier to deal with the constraint of divergence-free condition. Our method is based on employing the first-order edge element basis functions to expand the electric field and linear nodal element basis functions to expand the Lagrangian multiplier. Our numerical experiments show that this method can successfully remove all nonphysical zero and nonzero eigenvalues. We verify that when the cavity has a connected perfect electric boundary, then there is no physical zero eigenvalue. Otherwise, the number of physical zero eigenvalues is one less than the number of disconnected perfect electric boundaries.

1. INTRODUCTION

Waveguides and resonant cavities have wide applications in microwave engineering. Their design usually involves the computation of the propagation constants and resonant frequencies in computational electromagnetics [1]. For example, a very efficient technique for the full-wave analysis and design of complex passive waveguide filters, including rectangular cavities with metallic cylindrical posts and coaxial excitation, is presented in [2]. A homogeneous ferrite ring resonator and an inhomogeneous dielectric-ferrite ring resonator have been analyzed in [3]. However, in spite of their long history, such eigenvalue problems still require rigorous research in several aspects, especially with respect to the presence of two kinds of spurious modes, i.e., spurious nonzero eigenvalues and zero eigenvalues.

In 1969, Silvester [4] successfully employed the nodal based finite element method to analyze wave propagation in a homogeneous waveguide. It has been shown that the nodal based finite element method has several advantages in solving homogeneous waveguide problems, but when applied to inhomogeneous waveguide problems it yields nonphysical modes with nonzero eigenvalues. Rahman and Davies [5], Winkler and Davies [6] and Kobelansky and Webb [7] observed that the reason for the presence of these first-kind nonphysical modes is that these nonphysical modes do not satisfy the divergence-free condition required by the Gauss' law. They suggested a penalty function to enforce the divergence-free condition. Unfortunately, this method cannot eliminate the spurious modes completely and leaves the user the task of selecting a suitable penalty function parameter.

In electromagnetics theory [8, 9], we have already known that on the interface between two different media, the tangential component of electric field **E** is continuous, but the normal component is discontinuous. Because the nodal basis functions do not have this property, making use of nodal based finite element method to solve vector Maxwell's eigenvalue problem with inhomogeneous medium will lead to the presence of nonphysical nonzero eigenvalues. In 1980s, Nédélec [10, 11] proposed the edge

Received 26 May 2014, Accepted 19 July 2014, Scheduled 8 August 2014

* Corresponding author: Qing Huo Liu (qhliu@duke.edu).

[1] Institution of Electromagnetics and Acoustics, Xiamen University, Xiamen 361005, P. R. China. [2] LSEC, ICMSEC, Academy of Mathematics and Systems Science, Chinese Academy of Sciences, Beijing 100190, P. R. China. [3] Department of Electrical and Computer Engineering, Duke University, Durham, NC 27708, USA.

elements, which can preserve this actual physical property of electric field **E**. Therefore edge elements are very well suited for approximating electric field **E**. The review of edge element method has been given in [12]. For the Maxwell's eigenvalue problem in isotropic media, with the edge element method there are no spurious modes with nonzero eigenvalues, but the number of spurious modes with nonphysical zero eigenvalue is equal to the number of interior nodes inside the computational domain [13, 14]. Therefore, in order to remove these second-kind spurious modes with nonphysical zero eigenvalues, we must make the eigenfunction have the property of divergence-free condition. Kikuchi [15] has already turned to the help of introduction of Lagrangian multiplier to enforce the constraint of divergence-free condition. Other researchers have also investigated the removal of nonphysical zero eigenvalues [16, 17]. Kikuchi's approach [15] is particularly attractive in that the process is rather automatic with little intervention needed to include Gauss's law. However, to our knowledge, this method has only been applied to isotropic media so far; the extension to anisotropic media is not trivial in that it involves the coupling of all field components in the mass and stiffness matrices.

Fratalocchi et al. [18–20] concern the numerical solution of Maxwell equations in complex geometries. This paper will focus on numerical solving of 2D vector Maxwell eigenvalue problem with anisotropic media in complex geometries. Based on the above work by Kikuchi [15], we introduce a Lagrangian multiplier to constrain the divergence-free condition. Specifically, we employ the first order edge element basis functions to expand the electric field, and use linear nodal element basis functions to expand the Lagrangian multiplier so that Gauss' law is satisfied to remove the second-kind spurious modes.

The outline of the paper is as follows. In Section 2, we introduce the mixed variational formulation of the 2D vector Maxwell's eigenvalue problem in anisotropic media. Linear finite element space, the first order edge element space, and the forms of corresponding basis functions are given in Section 3. Finally we carry out some numerical experiments to verify that the mixed finite element method can effectively exclude all the spurious eigenvalues, including the nonphysical zero eigenvalues.

2. MIXED VARIATIONAL FORMULATION

In this work we consider the 2D electromagnetic eigenvalue problem for an anisotropic medium with the relative permittivity and relative permeability tensors

$$\bar{\bar{\epsilon}}_r = \begin{bmatrix} \bar{\bar{\epsilon}}_{rt} & 0 \\ 0 & \epsilon_{rz} \end{bmatrix}, \quad \bar{\bar{\mu}}_r = \begin{bmatrix} \bar{\bar{\mu}}_{rt} & 0 \\ 0 & \mu_{rz} \end{bmatrix}, \tag{1}$$

where $\bar{\bar{\epsilon}}_{rt}$ and $\bar{\bar{\mu}}_{rt}$ are full 2×2 tensors for the in-plane relative permittivity and permeability of the medium. In a 2D problem, all fields and medium properties are only functions of (x, y) and are independent of z.

Let Ω be a connected, bounded domain of $\mathbb{R}^2$ with a Lipschitz-continuous boundary $\partial\Omega$. The boundary $\partial\Omega$ may be disconnected. In a 2D resonant cavity problem, we often need to solve the following 2D vector Maxwell's eigenvalue problem: Find $k_0 \in \mathbb{R}$ (eigenvalue) and a vector field $\mathbf{E} \neq 0$ (eigenfunction) such that

$$\nabla_t \times \left(\mu_{rz}^{-1} \nabla_t \times \mathbf{E}\right) = k_0^2 \bar{\bar{\epsilon}}_{rt} \mathbf{E} \quad \text{in } \Omega, \tag{2}$$

$$\nabla_t \cdot \left(\bar{\bar{\epsilon}}_{rt} \mathbf{E}\right) = 0 \quad \text{in } \Omega, \tag{3}$$

$$\hat{n} \times \mathbf{E} = 0 \quad \text{on } \partial\Omega, \tag{4}$$

where $\hat{n}$ denotes the outward unit normal vector on $\partial\Omega$, $\nabla_t \times$ the curl operator, $\nabla_t \cdot$ the divergence operator, $\mathbf{E} = E_x \hat{x} + E_y \hat{y}$ the electric field in the 2D plane, $k_0^2 = \omega^2 \mu_0 \epsilon_0$, and ω the angular frequency. In this electromagnetic model, we only consider the perfect electric conductor (PEC) boundary condition, but the method can be extended to other boundary conditions. Moreover, we assume that the medium in resonant cavity is anisotropic and piecewise homogeneous, and in each region the relative dielectric permittivity $\bar{\bar{\epsilon}}_{rt}$ is a second order positive tensor, i.e.,

$$(\bar{\bar{\epsilon}}_{rt} \xi, \xi) = \xi^* \bar{\bar{\epsilon}}_{rt} \xi > 0 \quad \text{for} \quad \forall\, 0 \neq \xi \in \mathbb{C}^2, \tag{5}$$

where ξ^* is the complex conjugate of ξ, and the relative magnetic permeability $\mu_{rz} > 0$ is the zz component of the relative magnetic permeability tensor.

Note that when Ω is simply connected, i.e., the boundary $\partial\Omega$ is connected, the eigenvalue $k_0 = 0$ is not a solution of problem (2)–(4). In fact, if $k_0 = 0$, then the above problem has the trivial solution only: from (2) and (4), we can deduce that $\nabla_t \times \mathbf{E} = 0$, so we can write $\mathbf{E} = -\nabla_t\phi$. Substituting this into (3) and (4), we get the equation $-\nabla_t \cdot (\bar{\bar{\epsilon}}_{rt}\nabla_t\phi) = 0$ in Ω and ϕ is a constant on $\partial\Omega$, and using (5), we conclude that ϕ is the constant in Ω, thus, $\mathbf{E} = 0$ in Ω. On the other hand, when Ω is multiply connected, i.e., the boundary $\partial\Omega$ is disconnected, we cannot deduce $\mathbf{E} = -\nabla_t\phi$ from $\nabla_t \times \mathbf{E} = 0$; therefore, the presence of physical zero eigenvalue is possible. This is the case for a coaxial waveguide and for multi-conductor connectors. It is well known (and also confirmed by our numerical results) that the number of physical zero eigenvalue is equal to the genus in Ω. The physical interpretation for this is that if there are N independent conductors in this cavity, then there are $N-1$ independent TEM modes in this cavity. Unfortunately, numerical solution using the traditional finite element method will yield many spurious zero eigenvalues. Therefore, it is the objective of this work to remove these spurious modes by employing the mixed finite element method.

In order to use the mixed finite element method to solve this problem, we change the above strong form PDE to the corresponding weak form. Let $L_2(\Omega)$ be a Lebesgue space of measurable and square integrable functions on Ω. Its canonical inner product is defined as $(u, v)_0 = \int_\Omega uv^* d\Omega$, where the complex value function v^* stands for the complex conjugate function of v. The norm induced from the above inner product is $\|u\|_0 = \sqrt{\int_\Omega |u|^2 d\Omega}$. Let $L_2(\Omega)^2$ be the vector product space over two $L_2(\Omega)$ spaces. For any $\mathbf{J}, \mathbf{F} \in L_2(\Omega)^2$, $\mathbf{J} = J_x\hat{x} + J_y\hat{y}$, $\mathbf{F} = F_x\hat{x} + F_y\hat{y}$, the standard inner product and norm in $L_2(\Omega)^2$ can be defined as

$$(\mathbf{J}, \mathbf{F}) = \int_\Omega (J_x F_x^* + J_y F_y^*) d\Omega, \quad \|\mathbf{F}\| = \sqrt{(\mathbf{F}, \mathbf{F})}.$$

In the finite element postprocessing, for the problem (2)–(4) we need to draw field distribution about the electric field $\mathbf{E} = \hat{x}(E_x^{\text{real}} + jE_x^{\text{imag}}) + \hat{y}(E_y^{\text{real}} + jE_y^{\text{imag}})$. We denote $\text{Re}(\mathbf{E}) = \hat{x}E_x^{\text{real}} + \hat{y}E_y^{\text{real}}$, $\text{Im}(\mathbf{E}) = \hat{x}E_x^{\text{imag}} + \hat{y}E_y^{\text{imag}}$. Next we introduce the following three important Hilbert function spaces:

$$\begin{aligned} H_0^1(\Omega) &= \left\{q \in L_2(\Omega) : \nabla_t q \in L_2(\Omega)^2,\ q = 0 \text{ on } \partial\Omega\right\}, \\ \mathbf{H}(\text{curl}, \Omega) &= \left\{\mathbf{F} = F_x\hat{x} + F_y\hat{y} \in L_2(\Omega)^2 \colon \frac{\partial F_y}{\partial x} - \frac{\partial F_x}{\partial y} \in L_2(\Omega)\right\}, \\ \mathbf{H}_0(\text{curl}, \Omega) &= \left\{\mathbf{F} \in \mathbf{H}(\text{curl}, \Omega) \colon \hat{n} \times \mathbf{F} = 0 \text{ on } \partial\Omega\right\}. \end{aligned}$$

By applying the Green's formula

$$\int_\Omega \nabla_t \times \left(\mu_{rz}^{-1}\nabla_t \times \mathbf{E}\right) \cdot \mathbf{F} d\Omega = \int_\Omega \left(\mu_{rz}^{-1}\nabla_t \times \mathbf{E}\right) \cdot \nabla_t \times \mathbf{F} d\Omega + \int_{\partial\Omega} \left(\mu_{rz}^{-1}\nabla_t \times \mathbf{E}\right) \times \mathbf{F} \cdot d\mathbf{S},$$

to Equations (2), and

$$\int_\Omega \nabla_t \cdot \left(\bar{\bar{\epsilon}}_{rt}\mathbf{E}\right) q d\Omega = -\int_\Omega (\bar{\bar{\epsilon}}_{rt}\mathbf{E}) \cdot \nabla_t q d\Omega + \int_{\partial\Omega} q\,(\bar{\bar{\epsilon}}_{rt}\mathbf{E}) \cdot d\mathbf{S},$$

to Equation (3), and taking $\mathbf{F} \in \mathbf{H}_0(\text{curl}, \Omega)$, $q \in H_0^1(\Omega)$, we arrive at the following variational formulation of Maxwell's eigenvalue problem (2)–(4): Find $k_0^2 = \lambda \in \mathbb{R}$, $0 \neq \mathbf{E} \in \mathbf{H}_0(\text{curl}, \Omega)$ such that

$$\left(\mu_{rz}^{-1}\nabla_t \times \mathbf{E}, \nabla_t \times \mathbf{F}\right) = \lambda\left(\bar{\bar{\epsilon}}_{rt}\mathbf{E}, \mathbf{F}\right) \quad \forall \quad \mathbf{F} \in \mathbf{H}_0(\text{curl}, \Omega), \tag{6}$$

$$(\bar{\bar{\epsilon}}_{rt}\mathbf{E}, \nabla_t q) = 0 \quad \forall \quad q \in H_0^1(\Omega). \tag{7}$$

It is clear that Equation (6) can be solved independently as in the conventional edge element method, but in this case the divergence-free condition (3) may be not satisfied. Therefore, the problem (6) is not equivalent to the original problem (2)–(4). This is the reason that (6) has nonphysical zero eigenvalues, and the eigenfunction space corresponding to these nonphysical zero eigenvalues is $\nabla_t H_0^1(\Omega)$, which is an infinite dimensional space. When Maxwell's eigenvalue problem (2)–(4) does have several actual physical zero or very close to zero eigenvalues, it is very difficult to distinguish the actual physical zero eigenvalues from all the numerical eigenvalues to approximate these actual zero eigenvalues [21].

In order to exclude all the nonphysical zero eigenvalues, we need to consider the divergence-free condition (3). That is to say that we must simultaneously solve variational forms (6) and (7). We couple variational form (6) with that of (7) according to the introduction of Lagrangian multiplier and give the following mixed finite variational formulation: Seek $\lambda \in \mathbb{R}$, $0 \neq \mathbf{E} \in \mathbf{H}_0(\mathrm{curl}, \Omega)$, $p \in H_0^1(\Omega)$ such that

$$(\mu_{rz}^{-1}\nabla_t \times \mathbf{E}, \nabla_t \times \mathbf{F}) + (\bar{\bar{\epsilon}}_{rt}\mathbf{F}, \nabla_t p) = \lambda(\bar{\bar{\epsilon}}_{rt}\mathbf{E}, \mathbf{F}) \quad \forall \quad \mathbf{F} \in \mathbf{H}_0\,(\mathrm{curl}, \Omega), \tag{8}$$

$$(\bar{\bar{\epsilon}}_{rt}\mathbf{E}, \nabla_t q) = 0 \quad \forall \quad q \in H_0^1(\Omega), \tag{9}$$

where p is a Lagrangian multiplier. This is a saddle point problem in finite element analysis.

Now we prove the equivalence between the problem (6)–(7) and the problem (8)–(9). Obviously, any eigenpair of (6)–(7) with $p = 0$ satisfies (8)–(9). Conversely, by taking $\mathbf{F} = \nabla_t p$ in (8), we get $(\bar{\bar{\epsilon}}_{rt}\nabla_t p, \nabla_t p) = \lambda(\bar{\bar{\epsilon}}_{rt}\mathbf{E}, \nabla_t p)$. Then making use of (9) and (5), we deduce that $\nabla_t p = 0$. By means of the property of Hilbert space $H_0^1(\Omega)$ [22], we can deduce $p = 0$ in Ω, which shows that any eigenpair of (8)–(9) satisfies Equations (6)–(7) as well. Next we use the mixed finite element method to discretize the mixed variational problem (8)–(9).

3. MIXED FINITE ELEMENT DISCRETIZATION

In this section, we will describe two important finite element spaces: one is the nodal-based scalar linear element space S_h, which is a scalar function space; the other is the first order edge-based vector element space W_h.

Let π_h be a regular triangulation [22] of Ω with the mesh parameter h, where h stands for the length of the longest edge in triangular mesh π_h. The usual definition of a linear element space S_h is

$$S_h = \left\{\phi \in H_0^1(\Omega)\colon \phi|_K \in P_1(K),\ \forall\ K \in \pi_h\right\},$$

where $P_1(K)$ is the first order polynomial space on K, and the local basis functions in S_h are called nodal basis functions because the degree of freedom is defined on the nodes of the mesh. Let φ_i^K $(1 \leq i \leq 3)$ be these three local nodal basis functions on the element K.

Here we only consider the first order edge element space W_h on a plane triangular mesh π_h.

Definition: The first order edge element is a triple $(K, \mathcal{P}, \mathcal{N})$ having the following properties:

(i) K is a triangle (element shape);

(ii) $\mathcal{P} = \{\mathbf{F}:\ \mathbf{F} = \hat{x}(a + by) + \hat{y}(c - bx)\}$ (shape function);

(iii) $\mathcal{N} = \left\{\int_{l_i} \mathbf{F} \cdot \tau_i ds,\ 1 \leq i \leq 3\right\}$ (degree of freedom),

where τ_i is the tangential unit vector of edge l_i.

The local edge element basis functions on a triangle can be expressed in terms of the nodal basis functions. According to the above definition, we can derive the concrete expressions of three local edge element basis functions, i.e.,

$$\begin{aligned}
\mathbf{N}_1^K &= \varphi_2^K \nabla_t \varphi_3^K - \varphi_3^K \nabla_t \varphi_2^K,\\
\mathbf{N}_2^K &= \varphi_1^K \nabla_t \varphi_3^K - \varphi_3^K \nabla_t \varphi_1^K,\\
\mathbf{N}_3^K &= \varphi_1^K \nabla_t \varphi_2^K - \varphi_2^K \nabla_t \varphi_1^K.
\end{aligned}$$

Figure 1 presents the local numbering of the nodes and edges of a triangle.

The definition of the first order edge element space W_h is

$$W_h = \left\{\mathbf{F} \in \mathbf{H}_0(\mathrm{curl}, \Omega)\colon \mathbf{F}|_K \in \mathrm{span}\{\mathbf{N}_1^K, \mathbf{N}_2^K, \mathbf{N}_3^K\},\ \forall\ K \in \pi_h\right\}.$$

Note that the directivity of the global basis function $\mathbf{N}_i$ in W_h associated with the i-th edge should be same as the reference direction. In our program, the global basis function $\mathbf{N}_i$ is directed from the lower to the higher global node number.

We use the first order edge element space W_h and the linear element space S_h to approximate the space $\mathbf{H}_0\,(\mathrm{curl}, \Omega)$ and $H_0^1\,(\Omega)$, respectively. Restricting (8)–(9) on $W_h \times S_h$, we obtain the discrete mixed variational formulation: Seek $\lambda_h \in \mathbb{R}$, $0 \neq \mathbf{E}_h \in W_h$, $p_h \in S_h$ such that

$$\left(\mu_{rz}^{-1}\nabla_t \times \mathbf{E}_h, \nabla_t \times \mathbf{F}\right) + (\bar{\bar{\epsilon}}_{rt}\mathbf{F}, \nabla_t p_h) = \lambda_h\,(\bar{\bar{\epsilon}}_{rt}\mathbf{E}_h, \mathbf{F}) \quad \forall \quad \mathbf{F} \in W_h, \tag{10}$$

$$(\bar{\bar{\epsilon}}_{rt}\mathbf{E}_h, \nabla_t q) = 0 \quad \forall \quad q \in S_h. \tag{11}$$

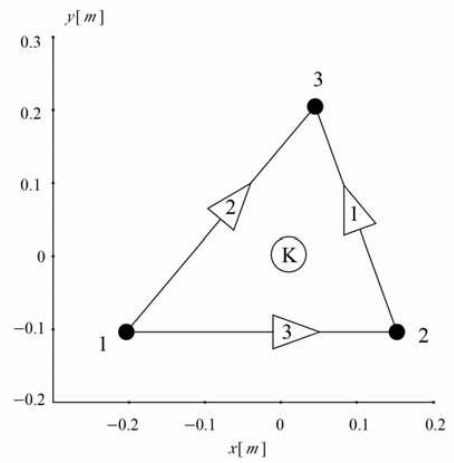

Figure 1. The local nodal numbering for the element K and the local reference direction for the edge are chosen by means of local nodal numbering.

Next we change Equations (10)–(11) to a matrix form. Suppose that $\mathbf{N}_1$, $\mathbf{N}_2$, ..., $\mathbf{N}_n$ are the global basis functions in W_h, where $n = \dim W_h$ is the number of interior edges in mesh π_h; ψ_1, ψ_2, ..., ψ_m are the global basis functions in S_h, where $m = \dim S_h$ is the number of interior nodes in mesh π_h. Since $\mathbf{E}_h \in W_h$ and $p_h \in S_h$, we can write

$$\mathbf{E}_h = \sum_{k=1}^{n} \xi_k \mathbf{N}_k, \quad p_h = \sum_{k=1}^{m} \zeta_k \psi_k. \tag{12}$$

Substituting (12) into (10)–(11), taking $\mathbf{F} = \mathbf{N}_k$ ($k = 1, 2, \ldots, n$), $q = \psi_k$ ($k = 1, 2, \ldots, m$), and setting $\xi = [\xi_1, \xi_2, \ldots, \xi_n]^T$, $\zeta = [\zeta_1, \zeta_2, \ldots, \zeta_m]^T$, we obtain the generalized matrix eigenvalue problem:

$$\begin{bmatrix} A & T \\ T^{\dagger} & O \end{bmatrix} \begin{bmatrix} \xi \\ \zeta \end{bmatrix} = \lambda_h \begin{bmatrix} M & O \\ O & O \end{bmatrix} \begin{bmatrix} \xi \\ \zeta \end{bmatrix}, \tag{13}$$

where $T^{\dagger}$ is conjugate transpose of matrix T,

$$\begin{aligned} A &= (a_{ij}) \in \mathbb{C}^{n\times n}, \quad T = (t_{ij}) \in \mathbb{C}^{n\times m}, \quad M = (m_{ij}) \in \mathbb{C}^{n\times n}, \\ m_{ij} &= (\bar{\bar{\epsilon}}_{rt}\mathbf{N}_j, \mathbf{N}_i), \quad t_{ij} = (\bar{\bar{\epsilon}}_{rt}\mathbf{N}_i, \nabla_t \psi_j), \\ a_{ij} &= \left(\mu_{rz}^{-1}\nabla_t \times \mathbf{N}_j, \nabla_t \times \mathbf{N}_i\right). \end{aligned}$$

After solving the generalized algebraic eigenvalue problem (13), we can get the distribution of the electric field in Ω using an interpolation technique.

Otherwise, we ignore the divergence-free condition (3), finally we get the following generalized eigenvalue problem:

$$A\xi = \lambda_h M\xi. \tag{14}$$

We see from our numerical results that the numerical eigenvalues of (14) have many zero eigenvalues (up to machine accuracy). Moreover, the finer the grid is, the more the zero eigenvalues from (14). In fact, the number of zero eigenvalue is equal to $\dim(S_h)$ when Ω is simply connected. In engineering practice, we often need to know the first few nonzero eigenvalues, if we make use of (14) to compute them directly, it is clear that this method is very time consuming and inefficient because the large null space of the curl-curl operator has not been removed, as illustrated in the following numerical experiments. Therefore the work of excluding these nonphysical zero eigenvalues is significant and important.

4. NUMERICAL EXPERIMENTS

In this section, we carry out several numerical experiments on the mixed finite element method and discuss the convergence property of numerical eigenvalues. The goals are to support that our method is

free of all the spurious modes and to compare the efficiency of this method with the conventional edge element method.

In order to analyze the convergence of the numerical Maxwell's eigenvalues, a simple method [14] is to perform computations for a geometric sequence of mesh parameter h such that $\frac{h_i}{h_{i+1}} = \frac{h_{i+1}}{h_{i+2}}$. Assuming that expansion of the eigenvalue is

$$\lambda_h = \lambda + Ch^\alpha + \dots. \tag{15}$$

One can then estimate the order of convergence as

$$\text{ratio}(\lambda_h) = \alpha = \ln\left[\frac{\lambda_{h_i} - \lambda_{h_{i+1}}}{\lambda_{h_{i+1}} - \lambda_{h_{i+2}}}\right] \Big/ \ln\left[\frac{h_i}{h_{i+1}}\right], \tag{16}$$

where the constant C is independent of h, and α is dependent on the regularity of the exact eigenfunction.

In fact, establishing the expansion of the eigenvalue (15) is a significant work, because we can use extrapolation method to improve the accuracy of numerical eigenvalues based on the asymptotic expansion (15). Suppose that

$$\lambda_{h/2,h}^{\text{extra}} = \frac{2^\alpha \lambda_{h/2} - \lambda_h}{2^\alpha - 1}.$$

We can know that $\lambda_{h/2,h}^{\text{extra}}$ is a numerical eigenvalue of high accuracy.

4.1. A Square Homogeneous Cavity

In order to verify the implementation of Equation (13), we first make a simulation for the easiest cavity. Suppose that the square cavity is with the length π m and the medium in this cavity is vacuum. We can solve the problem (2)–(4) analytically. The exact eigenvalues are $0 \neq \lambda_{mn} = m^2 + n^2$ $(m, n = 0, 1, 2, 3, 4, \dots)$ [21]. We compute the first five eigenvalues by using the mixed finite element and present the numerical results in Table 1. The extrapolation results of numerical eigenvalues are listed in Table 2.

Table 1. Numerical eigenvalues from a square isotropic homogenous cavity.

h	$\frac{\sqrt{2}\pi}{8}$	$\frac{\sqrt{2}\pi}{16}$	$\frac{\sqrt{2}\pi}{32}$	$\frac{\sqrt{2}\pi}{64}$	$\frac{\sqrt{2}\pi}{128}$	exact
λ_{1h}	0.992321	0.998066	0.999516	0.999879	0.999970	1.000000
λ_{2h}	0.999147	0.999795	0.999949	0.999987	0.999997	1.000000
λ_{3h}	2.008234	2.002121	2.000534	2.000134	2.000033	2.000000
λ_{4h}	3.931617	3.982881	3.995717	3.998930	3.999732	4.000000
λ_{5h}	3.932503	3.982939	3.995721	3.998930	3.999732	4.000000

Making use of (16), we can get the following order of the convergence:

$$\text{ratio}(\lambda_{1h}) \approx 1.994079, \quad \text{ratio}(\lambda_{2h}) \approx 2.029439, \quad \text{ratio}(\lambda_{3h}) \approx 1.976378,$$
$$\text{ratio}(\lambda_{4h}) \approx 1.998730, \quad \text{ratio}(\lambda_{5h}) \approx 1.991018.$$

From Table 1, we can observe that nonphysical zero eigenvalues are all removed effectively. The order of convergence for each numerical eigenvalue is approximately equal to 2. For the simple non-degenerate eigenvalues, the numerical eigenvalues approximate exact eigenvalues from above; however, for the multiply degenerate eigenvalues, the numerical eigenvalues approximate exact eigenvalues from below.

Remark: Note that for the easy model above, if we drop the divergence-free condition (3), then some nonphysical nonzero modes obtained by the finite element method with node-based element will be presented in numerical results, for details, please see [23]. However, our method can exclude these nonphysical nonzero modes effectively.

From Table 2, we can see that after the numerical extrapolation, the accuracy of numerical eigenvalues is improved dramatically. Here we take $\alpha = 2$ in the computation.

Table 2. The extrapolation of numerical eigenvalues from a square isotropic homogenous cavity.

h	$\frac{\sqrt{2}\pi}{8}, \frac{\sqrt{2}\pi}{16}$	$\frac{\sqrt{2}\pi}{16}, \frac{\sqrt{2}\pi}{32}$	$\frac{\sqrt{2}\pi}{32}, \frac{\sqrt{2}\pi}{64}$	$\frac{\sqrt{2}\pi}{64}, \frac{\sqrt{2}\pi}{128}$	exact
λ_1^{extra}	0.999980764677	0.999998781784	0.999999923601	0.999999995245	1.000000000000
λ_2^{extra}	1.000010461905	1.000000640137	1.000000039789	1.000000002516	1.000000000000
λ_3^{extra}	2.000083523329	2.000005172764	2.000000322519	2.000000020205	2.000000000000
λ_4^{extra}	3.999969167657	3.999996195386	3.999999731153	3.999999982710	4.000000000000
λ_5^{extra}	3.999750684919	3.999981781867	3.999998819890	3.999999925609	4.000000000000

Table 3. Numerical eigenvalues from a square anisotropic homogenous cavity.

h	$\frac{\sqrt{2}\pi}{8}$	$\frac{\sqrt{2}\pi}{16}$	$\frac{\sqrt{2}\pi}{32}$	$\frac{\sqrt{2}\pi}{64}$	$\frac{\sqrt{2}\pi}{128}$	trend
λ_{1h}	0.360110	0.361843	0.362324	0.362450	0.362483	$\nearrow$
λ_{2h}	0.851986	0.879173	0.886427	0.888271	0.888734	$\nearrow$
λ_{3h}	0.901434	0.892018	0.889671	0.889084	0.888938	$\searrow$
λ_{4h}	1.935574	1.907659	1.901324	1.899822	1.899455	$\searrow$
λ_{5h}	2.205845	2.354616	2.397779	2.409096	2.411969	$\nearrow$

If we change the medium parameters into an anisotropic ones,

$$\bar{\bar{\epsilon}}_{rt} = \begin{bmatrix} 2 & 1 \\ 1 & 2 \end{bmatrix}, \quad \mu_{rz} = 1,$$

for this resonant cavity, to our knowledge, the expression of the analytic solution is unknown, therefore we turn to the numerical method.

Making use of (16), we can obtain the following order of the convergence:

$$\text{ratio}(\lambda_{1h}) \approx 1.911929, \quad \text{ratio}(\lambda_{2h}) \approx 1.958429, \quad \text{ratio}(\lambda_{3h}) \approx 2.001947,$$
$$\text{ratio}(\lambda_{4h}) \approx 2.083227, \quad \text{ratio}(\lambda_{5h}) \approx 1.898175.$$

From Table 3, we can observe that nonphysical zero eigenvalues have also been removed effectively. The order of convergence for each numerical eigenvalue is also approximately equal to 2. The numerical eigenvalues approximate exact eigenvalues from above for some of the eigenvalues, but from below for others.

4.2. A Nonconvex Homogeneous Cavity

As we have already calculated the numerical eigenmodes of the cavity on a convex domain, now we consider Maxwell's eigenvalue problem for a nonconvex cavity. The geometrical shape of Ω and the initial mesh are presented in Figure 2(a). The medium parameters in this cavity are

$$\bar{\bar{\epsilon}}_{rt} = \begin{bmatrix} 1 & -j \\ j & 4 \end{bmatrix}, \quad \mu_{rz} = 1.$$

The numerical solution obtained by the mixed finite element method is as Table 4.

Because of the influence from round-off error in computer, we find that our numerical eigenvalues are all complex, but their imaginary parts are very small (about 10^{-12}). Here we only list the real parts.

By applying (16), we can get the following order of the convergence:

$$\text{ratio}(\lambda_{1h}) \approx 1.313748, \quad \text{ratio}(\lambda_{2h}) \approx 1.308231, \quad \text{ratio}(\lambda_{3h}) \approx 1.255196,$$
$$\text{ratio}(\lambda_{4h}) \approx 1.289295, \quad \text{ratio}(\lambda_{5h}) \approx 1.384481.$$

As observed from Table 4, all nonphysical zero eigenvalues have been removed effectively and the order of convergence for each numerical eigenvalue is approximately equal to 1.3, which is less than that

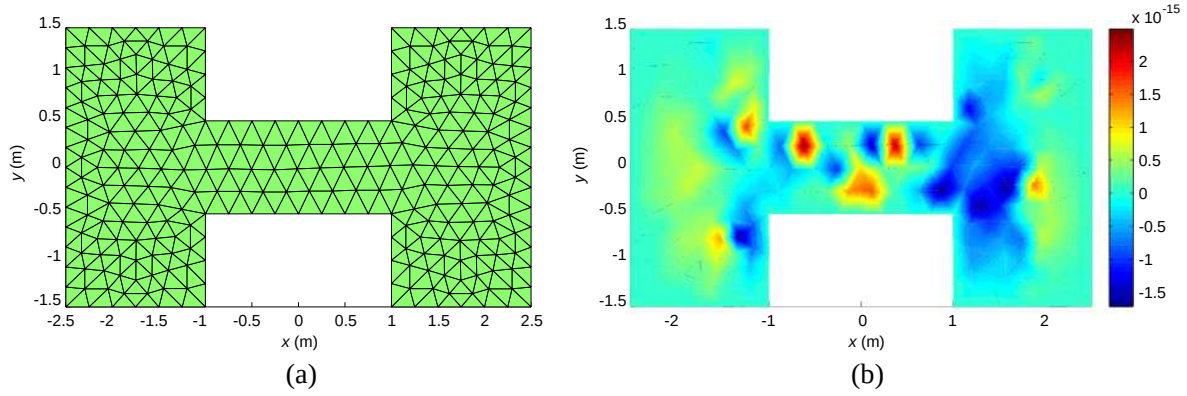

Figure 2. A homogenous nonconvex cavity. (a) The initial mesh and geometrical shape. (b) The distribution of function values of the Lagrange multiplier p_h corresponding to the first numerical eigenvalue $\lambda_{1h} = 0.040378$ on the first mesh in Table 4.

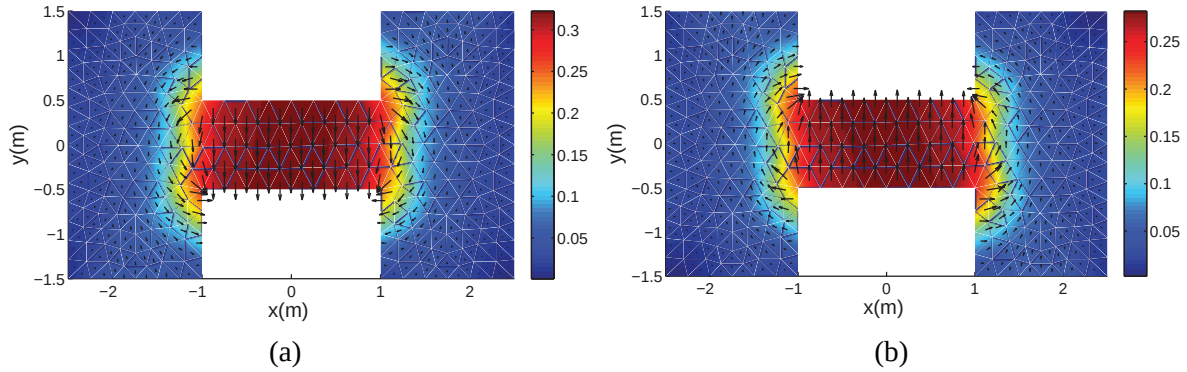

Figure 3. The field distribution in the nonconvex cavity corresponding to the first numerical eigenvalue $\lambda_{1h} = 0.040378$ on the first mesh. (a) Magnitude and field distribution of $\mathrm{Re}(\mathbf{E}_h)$. (b) Magnitude and field distribution of $\mathrm{Im}(\mathbf{E}_h)$.

Table 4. Numerical eigenvalues from a nonconvex anisotropic homogenous cavity.

h	0.293524	0.146762	0.073381	0.036690	0.018345	trend
λ_{1h}	0.040378	0.040884	0.041091	0.041173	0.041206	↗
λ_{2h}	0.388638	0.395901	0.398877	0.400074	0.400552	↗
λ_{3h}	0.781945	0.784755	0.785987	0.786498	0.786704	↗
λ_{4h}	0.982714	0.992164	0.996140	0.997754	0.998401	↗
λ_{5h}	1.606289	1.626574	1.634283	1.637230	1.638369	↗

in the above two examples. The main reason for this lower convergence speed is the bad smoothness of the eigenfunction on nonconvex domain due to the singular behavior of the electric field [24–26]. The distributions of real and imaginary part of electric field corresponding to the first numerical eigenvalue are presented in Figure 3, where one can find that the electric field distribution in the middle of this nonconvex cavity is uniform. From Figure 2(b), we can conclude that the function values of the Lagrange multiplier p_h on the nodes of the mesh are very small, this is in accordance with the theory in Section 2.

In summary, from Tables 1–4, resonant cavities are all simply connected (i.e., only one perfect electric conductor in the problem) and there are no any physical zero eigenvalues, thus confirming the advantage of the mixed finite element method, whereas there are many spurious nonphysical zero eigenvalues in the traditional edge element method.

4.3. A Coaxial Cavity

Next, we consider the Maxwell's eigenvalue problem for a coaxial cavity, the domain is

$$\Omega = \left\{(x, y)\colon a^2 < x^2 + y^2 < b^2\right\},$$

where a and b are inner and outer radii of this PEC coaxial cavity, respectively. We assume that the medium parameters of this cavity are

$$\bar{\bar{\epsilon}}_{rt} = \begin{bmatrix} 2 & 2j \\ -2j & 3 \end{bmatrix}, \quad \mu_{rz} = 3,$$

we calculate this model with $a = 1\,\text{m}$ and $b = 2\,\text{m}$ by means of the mixed finite element method. The first five numerical eigenvalues from the mixed finite element method are listed in Table 5.

Here we only list the real parts of our numerical eigenvalues because their imaginary parts are also very small. Making use of (16), we can obtain the following order of the convergence:

$$\text{ratio}(\lambda_{2h}) \approx 1.965949, \quad \text{ratio}(\lambda_{3h}) \approx 1.979530,$$
$$\text{ratio}(\lambda_{4h}) \approx 2.000355, \quad \text{ratio}(\lambda_{5h}) \approx 1.949117.$$

From Table 5, we observe that all nonphysical zero eigenvalues are also removed effectively, but we find the existence of one physical numerical zero eigenvalue with algebraic multiplicity one. The order of convergence for each numerical eigenvalue (exclude zero eigenvalue) is approximately equal to 2. The field distribution of the eigenfunction corresponding to this zero eigenvalue is shown in Figure 4.

Table 5. Numerical eigenvalues from an anisotropic homogenous coaxial cavity.

h	0.624198	0.312099	0.156050	0.078025	0.039012	trend
λ_{1h}	1.94e-16	−4.16e-17	1.45e-14	−4.14e-15	−9.40e-13	
λ_{2h}	0.053059	0.052738	0.052654	0.052632	0.052627	↘
λ_{3h}	0.071420	0.072896	0.073278	0.073374	0.073399	↗
λ_{4h}	0.201448	0.198993	0.198380	0.198227	0.198188	↘
λ_{5h}	0.294931	0.311180	0.315591	0.316716	0.316998	↗

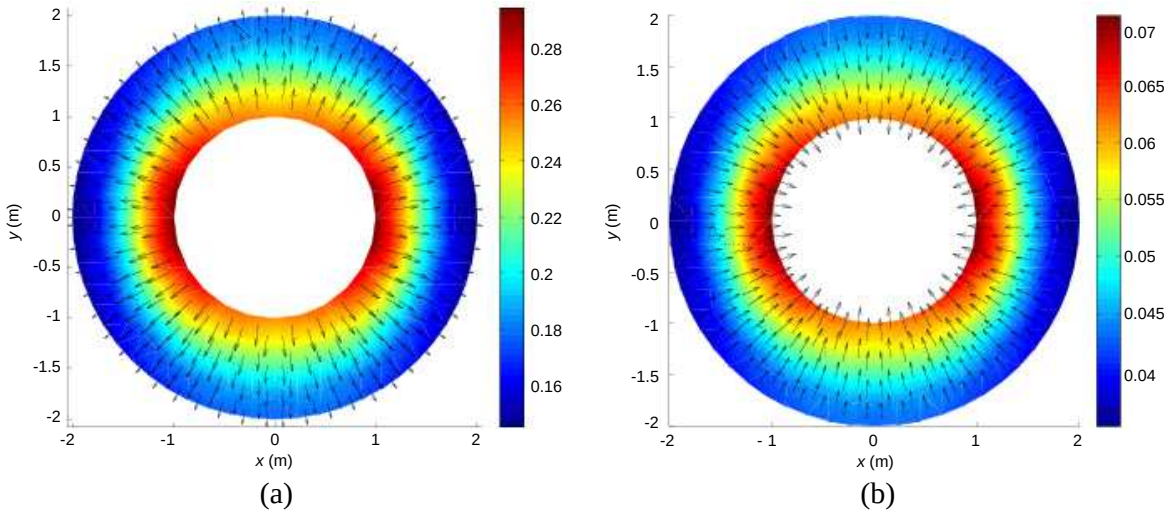

Figure 4. The field distribution in the anisotropic coaxial cavity corresponding to numerical zero eigenvalue on the second mesh. (a) Magnitude and field distribution of $\text{Re}(\mathbf{E}_h)$. (b) Magnitude and field distribution of $\text{Im}(\mathbf{E}_h)$.

4.4. An Anisotropic Inhomogeneous Cavity

Finally, we consider the resonant PEC cavity with an anisotropic inhomogeneous medium. Suppose that $\Omega_1 = \{(x,y) : (x+1)^2 + y^2 < \frac{1}{9}\}$, $\Omega_2 = \{(x,y) : (x-1)^2 + y^2 < \frac{1}{9}\}$, $\Omega_3 = [-2,0] \times [-1,1] \backslash \Omega_1$, $\Omega_4 = [0,2] \times [-1,1] \backslash \Omega_2$, and $\Omega = \Omega_3 \bigcup \Omega_4$. We assume that the medium parameters of this cavity are

$$\bar{\bar{\epsilon}}_{rt}^{(1)} = \begin{bmatrix} 1 & 0 \\ 0 & 2 \end{bmatrix}, \quad \mu_{rz}^{(1)} = 1 \text{ in } \Omega_3; \quad \bar{\bar{\epsilon}}_{rt}^{(2)} = \begin{bmatrix} 3 & -2j \\ 2j & 8 \end{bmatrix}, \quad \mu_{rz}^{(2)} = 3 \text{ in } \Omega_4,$$

The numerical results by employing the mixed finite element method are listed in Table 6.

Here we only list real part of our numerical eigenvalues because their imaginary parts are very small and in fact negligible. We can obtain the following order of the convergence:

$$\text{ratio}(\lambda_{3h}) \approx 1.702567, \quad \text{ratio}(\lambda_{4h}) \approx 1.900009, \quad \text{ratio}(\lambda_{5h}) \approx 1.646640.$$

All nonphysical zero eigenvalues are also removed effectively in Table 6; however, we also find the existence of a numerical physical zero eigenvalue with algebraic multiplicity two due to there are two PEC bodies in this cavity. The field distributions of the eigenfunction corresponding to the first and second numerical zero eigenvalue are shown in Figure 5 and Figure 6, respectively. All the numerical eigenvalues (exclude two zero eigenvalues) approximate the exact eigenvalues from below. For this cavity with an inhomogeneous medium, the order of convergence for different nonzero numerical eigenvalues may be different.

In order to compare the computational cost of the method in this paper and the conventional edge element method, we choose the numerical example above as a testing for CPU-time, and the results are listed in Table 7. Here t_1 and t_2 are the CPU times used by the mixed finite element method and by the conventional edge element method, respectively. In this testing, in order to get the first five smallest eigenvalues we only need to compute 5 numerical eigenvalues using mixed finite element method, however using conventional edge element method we need to compute $Np + 5$ numerical eigenvalues, where Np is the number of internal nodes in the mesh. When the mesh is fine, Np is very large.

Table 6. Numerical eigenvalues from an anisotropic inhomogeneous cavity.

h	0.500000	0.250000	0.125000	0.062500	0.031250	trend
λ_{1h}	3.47e-17	−1.90e-15	−5.11e-14	1.59e-14	−2.49e-13	
λ_{2h}	2.75e-15	−7.94e-15	−5.76e-14	−5.94e-13	−8.49e-12	
λ_{3h}	0.051665	0.051786	0.051826	0.051838	0.051841	↗
λ_{4h}	0.198117	0.203130	0.204541	0.204915	0.205012	↗
λ_{5h}	0.244447	0.246219	0.246868	0.247068	0.247126	↗

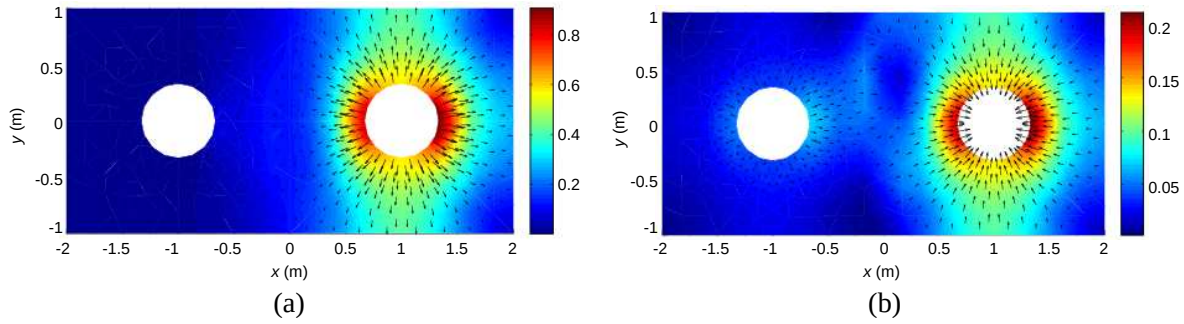

Figure 5. The field distribution in the anisotropic inhomogeneous cavity corresponding to the first numerical zero eigenvalue on the second mesh. (a) Magnitude and field distribution of $\text{Re}(\mathbf{E}_h)$. (b) Magnitude and field distribution of $\text{Im}(\mathbf{E}_h)$.

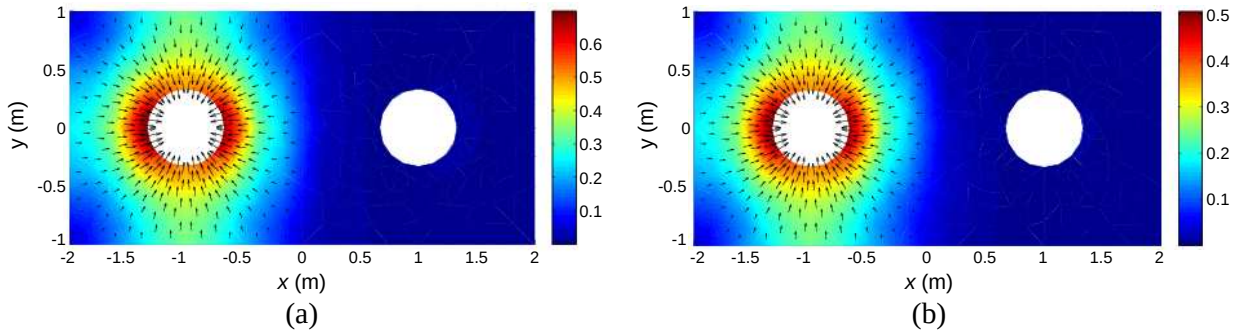

Figure 6. The field distribution in the anisotropic inhomogeneous cavity corresponding to the second numerical zero eigenvalue on the second mesh. (a) Magnitude and field distribution of $\mathrm{Re}(\mathbf{E}_h)$. (b) Magnitude and field distribution of $\mathrm{Im}(\mathbf{E}_h)$.

Table 7. The CPU-time of two methods.

h	0.500000	0.250000	0.125000	0.062500	0.031250
t_1 (second)	0.093600	0.296402	0.452403	1.653611	10.14006
t_2 (second)	0.421203	10.59247	920.8437	-	-

We can also see that the nonzero numerical eigenvalues using the mixed finite element method in this paper are the same as the ones using conventional edge element method, and the function values of the Lagrange multiplier p_h on the nodes of the mesh are very small, which agrees with the theory in Section 2. Furthermore, we also use the commercial software COMSOL Multiphysics to stimulate all the numerical examples above. When the eigenvalue is nonzero, our numerical results are also in excellent agreement with the ones from COMSOL Multiphysics. Note that COMSOL Multiphysics makes use of conventional edge element method to solve the vector Maxwell's eigenvalue problem, so it is clear that this method leads to the presence of nonphysical zero eigenvalues.

5. CONCLUSION

The 2D electromagnetic eigenvalue problem for a cavity filled with anisotropic media can be solved using the mixed finite element method. This method can exclude all the nonphysical zero and nonzero eigenvalues. If only a few eigenvalues are needed as in most engineering applications, this method is much more efficient than the conventional edge element method. In the future, we will extend the idea in this paper to 3D Maxwell's eigenvalue problem.

ACKNOWLEDGMENT

This work is supported by the National Natural Science Foundation of China (NSFC) under Grant 60931002 and Grant 41240029.

REFERENCES

1. Zhang, K. and D. Li, *Electromagnetic Theory for Microwaves and Optoelectronics*, Springer, Berlin Heidelberg, 2008.
2. Mira, F., A. A. San Blas, V. E. Boria, L. J. Roglá, and B. Gimeno, "Wideband generalized admittance matrix representation for the analysis and design of waveguide filters with coaxial excitation," *Radio Science*, Vol. 48, No. 1, 50–60, 2013.

3. Dillon, B. M. and A. A. P. Gibson, "Finite element solution of dielectric-ferrite resonators," *Radio Science*, Vol. 31, No. 5, 1191–1198, 1996.
4. Silvester, P., "Finite element solution of homogeneous waveguide problems," *Alta Frequenza*, Vol. 38, 313–317, 1969.
5. Rahman, B. M. and J. B. Davies, "Penalty function improvement of waveguide solution by finite elements," *IEEE Trans. on Microwave Theory and Tech.*, Vol. 32, 922–928, 1984.
6. Winkler, J. R. and J. B. Davies, "Elimination of spurious modes in finite element analysis," *J. Comput. Phys.*, Vol. 56, 1–14, 1984.
7. Kobelansky, A. J. and J. P. Webb, "Eliminating spurious modes in finite-element waveguide problems by using divergence-free fields," *Electron. Lett.*, Vol. 22, 569–570, 1986.
8. Chew, W. C., *Waves and Fields in Inhomogeneous Media*, Van Nostrand Reinhold, New York, 1990.
9. Balanis, C. A., *Advanced Engineering Electromagnetics*, Wiley, New York, 1989.
10. Nedelec, J. C., "Mixed finite elements in $\mathbb{R}^3$," *Numer. Math.*, Vol. 35, 315–341, 1980.
11. Nedelec, J. C., "A new family of mixed finite elements in $\mathbb{R}^3$," *Numer. Math.*, Vol. 50, 57–81, 1986.
12. Zhou, X. and G. Pan, "Application of physical spline finite element method (PSFEM) to fullwave analysis of waveguides," *Progress In Electromagnetics Research*, Vol. 60, 19–41, 2006.
13. Boffi, D., "Finite element approximation of eigenvalue problems," *Acta Numerica*, Vol. 19, 1–120, 2010.
14. Bondeson, A., T. Rylander, and P. Ingelstr, *Computational Electromagnetics*, Springer, New York, 2005.
15. Kikuchi, F., "Mixed and penalty formulations for finite element analysis of an eigenvalue problem in electromagnetism," *Comp. Meth. Appl. Mech. Engng.*, Vol. 64, 509–521, 1987.
16. Venkatarayalu, N. V. and J. F. Lee, "Removal of spurious DC modes in edge element solutions for modeling three-dimensional resonators," *IEEE Trans. on Microwave Theory and Tech.*, Vol. 54, 3019–3025, 2006.
17. Goncalves, M. S., F. J. Arnold, L. L. Bravo-Roger, and T. S. Santos, "A novel approach to suppress the DC modes in eigenvalue problems using the finite element method," *Microw. Opt. Techn. Lett.*, Vol. 55, 210–212, 2013.
18. Fratalocchi, A. and G. Ruocco, "Single-molecule imaging with X-ray free-electron lasers: Dream or reality?" *Phys. Rev. Lett.*, Vol. 106, 105504, 2013.
19. Gentilini, S., A. Fratalocchi, L. Angelani, G. Ruocco, and C. Conti, "Ultrashort pulse propagation and the Anderson localization," *Opt. Lett.*, Vol. 34, No. 2, 130–132, 2009.
20. Fratalocchi, A., C. Conti, and G. Ruocco, "Three-dimensional ab initio investigation of light-matter interaction in Mie lasers," *Physical Review A*, Vol. 78, 013806, 2008.
21. Brenner, S. C., F. Li, and L. Sung, "Nonconforming Maxwell eigensolvers," *J. Sci. Comput.*, Vol. 40, 51–85, 2009.
22. Ciarlet, P. G., "Basic error estimates for elliptic problem," *Handbook of Numerical Analysis, Volume II, Finite Element Methods (Part 1)*, Elsevier Science Publishers, North-Holland, 1991.
23. Boffi, D., P. Fernandes, L. Gastaldi, and I. Perugia, "Computational models of electromagnetic resonators: Analysis of edge element approximation," *SIAM J. Numer. Anal.*, Vol. 36, 1264–1290, 1999.
24. Costabel, M. and M. Dauge, "A remark on the regularity of solutions of Maxwell's equations on Lipschitz domains," *Math. Methods Appl. Sci.*, Vol. 12, 365–368, 1990.
25. Costabel, M. and M. Dauge, "Maxwell and Lamé eigenvalues on polyhedra," *Math. Methods Appl. Sci.*, Vol. 22, 243–258, 1999.
26. Costabel, M. and M. Dauge, "Singularities of electromagnetic fields in polyhedral domains," *Arch. Ration. Mech. Anal.*, Vol. 151, 221–276, 2000.